

Article ID: 1004-4140 (2007) 02-0052-08

## Low-dose CT Cardiac Imaging

Jiang Hsieh, John Londt, Melissa Vass,  
Xiangyang Tang, Jay Li, Darin Okerlund

(GE Healthcare, Milwaukee, WI 53201, USA)

**Abstract:** Cardiac imaging with computed tomography (CT) is one of the most recent advancements in CT clinical applications. Because of the low helical pitch employed in the cardiac acquisition protocols, radiation dose to patient is high. In this paper, we present a different data acquisition and image reconstruction technique that reduces dose to patient by 50%~89%. The key enabler for such technique is the large volume coverage (40 mm) of the 64-slice scanner. Compared to an average heart size of 120 mm to 140 mm the new VCT scanner is capable of covering the entire organ in 3 to 4 steps. In conjunction with the new acquisition, we present a complimentary reconstruction algorithm that overcomes incomplete projection samples. We conducted extensive phantom and clinical experiments to demonstrate the efficacy of the proposed approach.

**Keywords:** CT; cardiac imaging; step-and-shoot acquisition; cone beam reconstruction

**CLC number:** R322.1 R814.42

**Document code:** A

Two major technological advancements are key to the recent growth in cardiac applications, such as coronary artery imaging (CAI), with conventional CT scanners<sup>[1]</sup>. The first is the faster scan speed of the state-of-the-art scanners capable of rotating at 0.35s or faster per gantry rotation. Compared to a typical scan speed of one second per gantry rotation nearly a decade ago, this represents a factor of three improvement in terms of temporal resolution. Although the scan speed is still slower as compared to an electron beam scanner, advanced reconstruction algorithms partially compensate for some of the deficiencies. The second advancement is the introduction of multi-slice CT. State-of-the-art scanners collect up to 64 projections simultaneously. This allows a large portion of the heart to be scanned in a single rotation at a sub-millimeter slice thickness.

CAI acquisition relies on EKG signals to locate the quiescent phases of the heart. Many studies were conducted in the past to develop algorithms and protocols to reduce the impact of cardiac motion and to optimize image quality<sup>[2-13]</sup>. To ensure that the reconstruction is performed at the same phase in a cardiac cycle, reconstruction window is selected at identical locations relative to the R-to-R interval of the EKG. Low-pitch helical mode is typically employed to guarantee that the entire heart volume is properly covered. For illustration, we plot the detector row position as a function of time in Fig.1. In this figure, different cardiac cycles are separated by horizontal dotted lines and the detector-row locations are depicted by the solid diagonal lines. Every point on these lines represents a single-row projection collected at a

certain  $z$  location and a particular time (therefore a particular projection angle). For simplicity of illustration, we depict a four-row scanner. The shaded boxes in the figure show the temporal windows of the reconstructed images. These boxes, therefore, depict a unique set of time intervals and  $z$ -locations. Width of the box represents the volume in  $z$  that can be covered with reconstructions corresponding to a particular cardiac cycle. If the combination of gantry speed and helical pitch is not properly selected, the entire heart volume will not be uniformly covered in the reconstructed images. For example, if the table travels too fast (helical pitch is too high), gaps are present between adjacent volumes as shown in the figure. Although small gaps can be filled by image space interpolation, larger gaps will lead to discontinuities and artifacts in the volume rendered images. This is particularly problematic when considering the heart rate variation in a typical patient.

To ensure complete volume coverage, helical pitches between 0.1 and 0.3 are commonly used to account for the worst-case scenario. This translates to a higher dose to patients since the x-ray is continuously turned on and regions exposed to the x-ray radiation are highly overlapped. One of the methods of dose reduction is the use of mA-modulation where the x-ray tube current is modulated such that the x-ray flux is reduced outside the reconstruction window. Despite of these efforts, cardiac imaging remains to be one of the highest x-ray dose applications in CT. In this paper, we present a different acquisition technique that allows significant reduction of x-ray dose to patient. Due to the non-uniform coverage of the scanned volume, a complimentary reconstruction technique is developed to ensure the fidelity of the reconstructed images.

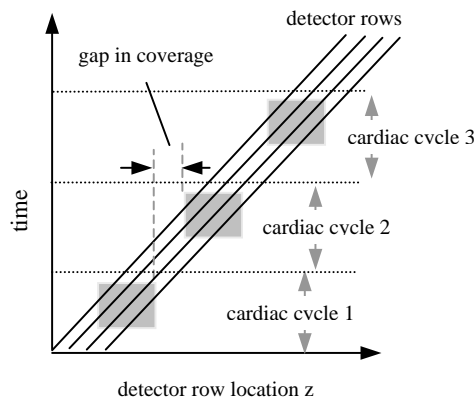


Fig.1 Illustration of coverage gap due to inappropriate helical pitch selection

## I. DATA ACQUISITION AND RECONSTRUCTION

The key advantage of the helical scan is the elimination of the inter-scan delay (A patient is translated at a constant speed during the data acquisition). This feature, however, becomes a disadvantage in physiologically gated studies due to the high-dependency between the acquisition location and timing. Adjustment in the reconstruction window translates automatically to a shift in the reconstruction location in  $z$ .

With the introduction of 64-slice scanners, the volume coverage is significantly increased as compared to a 16-slice scanner. For example, a LightSpeed<sup>16</sup> detector covers only 10 mm in  $z$  at iso-center when acquiring in 0.625 mm mode, while LightSpeed VCT<sup>64</sup> covers 40 mm. Compared to a typical heart size of 12 to 140 mm the 64-slice scanner is capable of covering the entire heart in 3 to 4 steps, as shown in Fig.2. Considering inter-scan delays of roughly one second, the total non-data acquisition period due to inter-scan delay in a cardiac study is no

longer prohibitive and helical acquisition is no longer a necessity. As a result, step-and-shoot data acquisition (SAS) becomes a viable candidate. In SAS mode, the patient remains stationary during the data acquisition of a cardiac cycle and moves to the next heart location during the subsequent cardiac cycles.

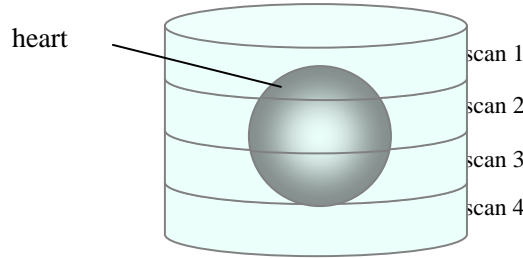


Fig.2 Illustration of step-and-shoot cardiac scan

For analysis, let us compare the acquisition time at a gantry speed of 0.4s per rotation. Helical data acquisition completes a CAI study in roughly 5s. If SAS mode is used, the study can be completed in 7s. A recent study of over 90 EKG signals has shown that by reducing the data acquisition time from 20s to 7s, the standard deviation in heart rate reduces from 5.74 to 4.54, a 20% reduction. This translates directly to an improved image quality and reduced motion artifacts. As the detector coverage increases, the acquisition time difference between the two scan modes reduces. When the volume coverage is sufficiently large, the SAS acquisition will be superior to the helical mode in terms of acquisition time<sup>[17]</sup>.

There are several advantages of the proposed scan protocol. The first is the improved ability to deal with arrhythmia or irregular heart rate. During arrhythmia, the quiescent time period of the heart is significantly reduced or eliminated and the image quality during such cardiac cycles are significantly compromised. In a helical acquisition, we are forced to make a choice to either keep the images of suboptimal quality, or discard these images and leave a coverage gap. For SAS mode, the patient table does not index to the next location until a good dataset is collected. When abnormal EKG signal is detected, the scanner simply waits for the next cardiac cycle for data acquisition. This advantage comes from the separation of data acquisition timing and location in SAS mode.

The second advantage is the significantly reduced x-ray dose to patient. Note that x-rays are turned on only during the active data acquisition and reconstruction phases of the heart and turned completely off during other phases. Because of the data acquisition timing and location can be treated independently, the gating is more effective. Even for the case in which all cardiac phases need to be acquired and reconstructed, the SAS acquisition ensures that there is no x-ray exposure overlap in the covered regions. That is, all the regions are scanned only once, unlike the low-pitch helical case where majority of the volume is scanned multiple times.

Next, we perform a quantitative analysis on the dose reduction. For SAS acquisition, the dose,  $\xi_s$ , is proportional to the x-ray “on” time if we ignore the x-ray tube current modulation as a function of the projection angle to obtain more uniform noise:

$$\xi_s = c \cdot \alpha \cdot t_{rot} \cdot \left[ \frac{H}{d} \right] \quad (1)$$

where  $H$  is the heart size in  $z$ ,  $d$  is the detector  $z$ -coverage,  $t_{rot}$  is the gantry rotation period,  $\alpha$  is the angular coverage ratio of half-scan over full scan, and  $c$  is a factor that scales linearly with the x-ray tube current. For “regular-pitch” helical mode, we consider a modulated x-ray tube current as a function of the cardiac phase. It can be shown that the total dose,  $\xi_h$ , is:

$$\xi_h = c' \left( \left[ \frac{H}{d} \right] t_{hrt} + \alpha \cdot t_{rot} \right) + (c - c') \alpha \cdot t_{rot} \left[ \frac{H}{d} \right] \quad (2)$$

where  $c'$  is the scaling factor for tube current outside the systole or diastole phase, and  $t_{hrt}$  is the cardiac cycle. We use the ratio of the helical over SAS dose to understand the dose increase in helical mode (By definition, dose ratio is unity for SAS). The results are shown in Fig.3. It is clear from the figure that even for the 80% mA-modulation (lower tube current is 20% of the peak) and “regular pitch” helical, the dose saving of SAS is still more than a factor of two over a wide range of heart rates.

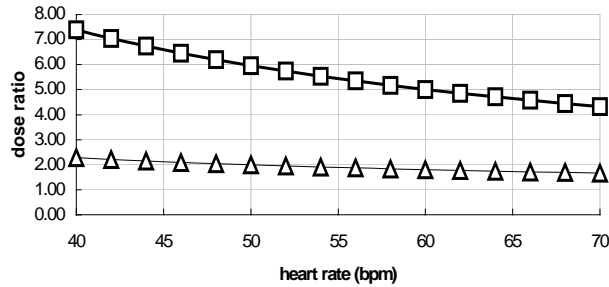


Fig.3 Helical dose ratio relative to SAS mode  
squares: “regular pitch” helical without mA modulation  
triangles: “regular pitch” helical with 80% modulation

Let us now consider the reconstruction algorithm. To improve temporal resolution, half-scan is typically used in image reconstruction. In half-scan mode, projections over the projection angle of  $\pi + 2\gamma_m$  are used instead of  $2\pi$ , where  $\gamma_m$  is the fan angle of the detector. A FDK-based reconstruction formula can be described by the following equation<sup>[14]</sup>:

$$f(x, y, z) = \frac{1}{2} \int_0^{\pi + 2\gamma_m} \left( \frac{D}{D + y'} \right)^2 d\beta \times \int_{-\infty}^{\infty} \frac{D}{\sqrt{D^2 + s^2 + v^2}} w(s, \beta) q(s, v, \beta) h(s' - s) ds \quad (3)$$

where  $w(s, \beta)$  is the well-known half-scan weight<sup>[15]</sup>:

$$w(s, \beta) = 3\theta^2(\gamma, \beta) - 2\theta^3(\gamma, \beta) \quad (4)$$

and

$$\theta(\gamma, \beta) = \begin{cases} \frac{\beta}{2\gamma_m - 2\gamma}, & 0 \leq \beta < 2\gamma_m - 2\gamma, \\ 1, & 2\gamma_m - 2\gamma \leq \beta < \pi - 2\gamma, \\ \frac{\pi + 2\gamma_m - \beta}{2\gamma_m + 2\gamma}, & \pi - 2\gamma \leq \beta < \pi + 2\gamma_m. \end{cases}$$

Here,  $D$  is the source to iso-center distance,  $s$  and  $v$  are the projection channel and row locations corresponding to the reconstructed pixel  $(x, y, z)$ ,  $\beta$  is the projection angle, and  $\gamma$  is the detector fan angle corresponding to  $s$ .

For step-and-shoot acquisition mode, it is well known that the completely sampled region is less than a cylindrical disc with its height equal to the detector iso-center coverage<sup>[16]</sup>. The cone beam geometry reduces the coverage of each projection to a region with its height much narrower than the desired volume near the source, as shown in Fig. 4. Although in theory one can reduce the reconstructed volume to the smallest coverage of the cone beam to avoid missing samples, it results in an unnecessary increased dose to patient. Note that for a typical CT scanner geometry, a 46% reduction in the reconstructed volume will result. To overcome this difficulty, we propose the following approach. Because of the cone beam geometry, the region closer to the detector covers a z-extent that is significantly higher than the coverage at iso. Therefore, if we consider two projections that are spaced one detector width (at iso) apart and their projection angles differ by  $\pi$ , there is little sampling gap in the reconstructed volume. The two projections, therefore, form a complimentary pair.

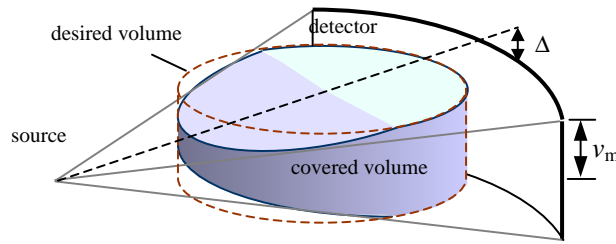


Fig.4 Reduction in coverage due to cone beam geometry

In the reconstruction process, we combine the contributions of neighboring halfscans to compensation for the missing sampling regions in any halfscan alone. The projection dataset first undergoes a row-by-row fan-to-parallel beam rebinning. For each projection sample,  $p_A(s, v, \beta)$ , we examine the neighboring projection sample,  $p_B(s', v', \beta')$ , where  $|\beta' - \beta| = n\pi$  with  $n$  being an odd integer. By comparing  $v$  and  $v'$ , a weighting function,  $\xi_A(x, y, z)$ , is defined during the backprojection step of the reconstruction:

$$\xi_A(x, y, z) = \frac{\varepsilon_A(x, y, z)}{\varepsilon_A(x, y, z) + \varepsilon_B(x, y, z)} \quad (5)$$

The reconstruction equation is given by:

$$f_A(x, y, z) = \frac{1}{2} \int_0^{\pi+2\gamma_m} \left( \frac{D}{D+y'} \right)^2 \xi_A(x, y, z) d\beta \times \int_{-\infty}^{\infty} \frac{D}{\sqrt{D^2 + s^2 + v^2}} w(s, \beta) q(s, v, \beta) h(s' - s) ds \quad (6)$$

Similar calculations are carried out for the adjacent scan that produces image  $f_B(x, y, z)$ . The final image,  $f(x, y, z)$ , is then the summation of the neighboring reconstructions:

$$f(x, y, z) = f_A(x, y, z) + f_B(x, y, z) \quad (7)$$

## II. EVALUATION

To evaluate the proposed reconstruction algorithm, we performed computer simulations, phantom experiments, and clinical studies. The goal of the experiment is to ensure that the proposed reconstruction algorithm produces equivalent image quality as the traditional helical scan acquisition under normal heart rate conditions. We first performed phantom experiments with a water-filled balloon that inflates and deflates triggered by an EKG signal. The phantom

was scanned with both helical and step-and-shoot mode. Little difference can be observed in terms of image quality. We then scanned various stationary phantoms of more complex structures to evaluate cone beam effects. Again, comparable image quality was obtained with both modes.

For clinical evaluation, patients were scanned with both helical and SAS modes and reformatted images were reconstructed for the entire heart volume. One such example is shown in Fig.5. It is clear from the figure that the image quality of both acquisition modes is comparable.

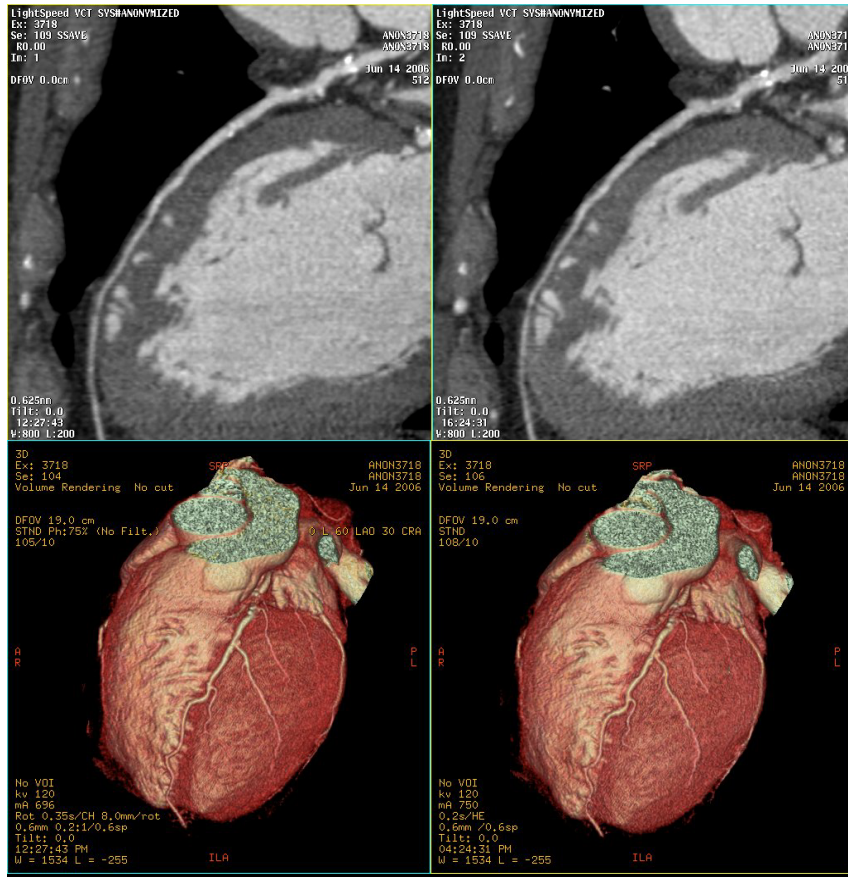


Fig.5. Clinical comparison of helical (left) and SAS (right) scan techniques

Next, we evaluate the dose saving of the SAS protocol as compared to the helical mode. The results for prospectively gated axial scans evaluated with  $\pm 5\%$  and  $\pm 10\%$  confidence margins and the retrospectively gated helical scans evaluated with routine EKG modulated mA (70%~80% R-to-R full mA, lowering to 20% of peak mA elsewhere) are shown in Table 1. The results show that a significant dose reduction was achieved using the SAS scan mode. Similar evaluation was carried out between the SAS mode and helical mode without mA-modulation. Dose savings between 73% and 89% were achieved.

Table 1 Dose comparison for SAS scans (500mA) and helical scans (450mA) with routine EKG modulated mA (70%~80% R-to-R full mA, 20% of peak mA elsewhere).

HR	Helical Dose /mSv	$\pm 10\%$ confidence margin			$\pm 5\%$ confidence margin		
		Margin/ms	SAS Dose /mSv	Percent Dose Reduction	Margin/ms	Dose/mSv (cine)	Percent Dose Reduction
40	13.2	150	5.8	56%	75	4.2	68%
45	11.5	150	5.8	49%	75	4.2	63%
50	11.0	125	5.3	52%	62.5	3.9	64%
55	11.1	125	5.3	52%	62.5	3.9	65%
60	10.7	100	4.7	56%	50	3.7	66%
65	10.5	100	4.7	55%	50	3.7	65%

### III. CONCLUSION

In this paper, we present a step-and-shoot (SAS) acquisition and reconstruction approach for cardiac CT imaging. Compared to the traditional helical acquisition mode, the proposed approach has the advantage of improved ability to handle arrhythmia or irregular heart rate and a significantly reduced dose to patient. The first advantage comes from the fact that in SAS mode, the data acquisition timing and location is independent. This is in contrast to the helical mode in which a shift in the temporal acquisition window means an adjustment in the data acquisition location in  $z$ . The second advantage comes from the fact that overlapped x-ray exposure to patient can be eliminated in the SAS mode. Compared to the helical mode without x-ray tube current modulation, a 73%~89% dose saving can be achieved. Even for helical scans with 70%~80% tube current modulation, the dose saving is still more than 50%.

Because of the cone beam geometry and the use of half-scan reconstruction, the reconstructed volume is not completely samples in all regions. To overcome this shortcoming, we propose a reconstruction algorithm that makes use of complimentary samples in the adjacent scans. The proposed reconstruction algorithm employs a weighting function to ensure the contribution to the final image is scaled with the quality of the data. Extensive computer simulation, phantom experiments, and clinical evaluations were conducted. Results have shown that the proposed reconstruction provides excellent image quality comparable to that obtained with the helical scan mode.

### REFERENCES

- [1] Hsieh J, Computed Tomography, principles, design, artifacts, and recent advances, SPIE press, 2002.
- [2] Herzog C, Abolmaali N, Balzer JO, et al. Heart-rate-adapted image reconstruction in multidetector-row cardiac CT: influence of physiological and technical prerequisite on image quality[J]. Eur Radiol, 2002, 12(11): 2670-2678.

- [3] Taguchi K, Anno H. High temporal resolution for multislice helical computed tomography[J]. *Med Phys* 2000,27(5): 861-872.
- [4] Choi H S, Choi B W, Choe K O, et al. Pitfalls, artifacts, and remedies in multi-detector row CT coronary angiography[J]. *Radiographics*, 2004, 24(3): 787-800.
- [5] Flohr T, Ohnesorge B, Bruder H et al. Image reconstruction and performance evaluation for ECG-gated spiral scanning with a 16-slice CT system[J]. *Med Phys*, 2003, 30(10): 2650-2662.
- [6] Saito K, Saito M, Komatsu S, et al. Real-time four-dimensional imaging of the heart with multi-detector row CT[J]. *Radiographics*, 2003, 23(1): 8.
- [7] Manzke R, Grass M, Hawkes D. Artifact analysis and reconstruction improvement in helical cardiac cone beam CT[J]. *IEEE Trans Med Imag*, 2004, 23(9): 1150-1164.
- [8] Pack J D, Noo F, Kudo H. Investigation of saddle trajectories for cardiac CT imaging in cone-beam geometry[J]. *Phys Med Biol*, 2004, 49(11): 2317-2336.
- [9] Kachelrieß M, Kalender W A. Electrocardiogram-correlated image reconstruction from sub-second spiral computed tomography scans of the heart[J]. *Med Phys*, 1998, 25: 2417-2431.
- [10] Hsieh J, Pan T, Acharya K C, et al. Non-uniform phase coded image reconstruction for cardiac CT[J]. *Radiology* 1999, 213: 401.
- [11] Hsieh J, Mayo J, Archarya K C, et al. Adaptive phase-coded reconstruction for cardiac CT[C]. *Proc SPIE Med Imaging* 2000.
- [12] Woodhouse C E, Janowitz W R, Viamonte M, Coronary arteries: retrospective cardiac gating technique to reduce cardiac motion artifact at spiral CT[J]. *Radiology*, 1997, 204: 566-569.
- [13] McCollough C H, Kaufmann R B, Cameron B M, et al. Electron-beam CT: use of a calibration phantom to reduce variability in calcium quantitation[J]. *Radiology*, 1995, 196: 159-165.
- [14] Feldkamp L A, Davis L C, Kress J W. Practical cone-beam algorithm[J]. *J Opt Soc Am A*, 1984, 1: 612-619.
- [15] Parker D L. Optimization of short scan convolution reconstruction and fan beam CT[C]. *Proc Int Workshop on Phys Engr Med Imag*, 1982: 199-202.
- [16] Hsieh J. Reconstruction algorithm for single circular orbit cone beam scans[C]. *Proc IEEE Int Symp on Bio Imag*, 2002: 836-838.
- [17] Hsieh J, Londt J, Vass M, et al. Step-and-shoot data acquisition and reconstruction for cardiac computed tomography[J]. *Med Phys*, 2006, 33(11): 4236-4248.

**Biography:** Jiang Hsieh(1956 — ), male, got Ph. D. degree in Electrical and Computer Engineering Department, Illinois Institute of Technology, 1989. As a Adjunct Professor, Department of Medical Physics, University of Wisconsin at Madison, in 2004-present; as Chief Scientist, Manager, Applied Science Laboratory-CT, GE Healthcare Technologies, Milwaukee, Wisconsin. He published 140-papers and articles in international periodicals and important symposiums, 5 special books, and the authorization in the United States patents more than 120 pieces. E-mail: [jiang.hsieh@med.ge.com](mailto:jiang.hsieh@med.ge.com).



# Technique Advancements of Light Speed VCT and Its Clinical Applications

LI Jian-ying

(GE Healthcare Technologies, Beijing 100176, China)

**Abstract:** In this paper we introduced some of the technique advancements of GE Light Speed VCT in hardware, software and reconstruction algorithm areas, and how these advancements improved image quality and brought many advanced clinical applications into reality including 5-beat cardiac, emergency chest pain Triple Rule Out™ and total stroke work-up. We also discussed the need to balance image quality and X ray dose and what GE was doing to achieve the goal of getting diagnostic CT images at the lowest possible dose.

**Key words:** VCT; reconstruction algorithm; clinical applications; X ray dose

**作者简介:** 李剑颖 (1963—), 男。1990 年在美国杜克大学获得理学博士学位, 1990—1995 年在该校的医学院从事核医学成像基础研究。1995 年至今在通用电气公司 (GE) 医疗部工作。从事核医学临床研究、CT 系统研发和 CT 应用科学研究。目前任 GE 中国医疗部 CT 实验室首席科学家, 主要负责和临床专家合作进行临床应用、图像改进以及降低剂量等研究工作。E-mail: jianying.Li@med.ge.com。

(上接 59 页)

## 低剂量 CT 心脏成像

Jiang Hsieh, John Londt, Melissa Vass,  
Xiangyang Tang, Jay Li, Darin Okerlund

(通用电气医疗部 美国威斯康星州密尔沃基 53201)

**摘要:** 采用 CT 进行心脏成像是 CT 临床应用中最前沿的进展, 心脏扫描中采用较低的螺距使得病人的辐照剂量较高, 我们提出一种不同的数据采集和图像重建技术, 使病人的辐照剂量减少了 50%~89%。该方法的使能技术是 64 排 CT 的大容积覆盖范围 (40 mm), 相对于心脏的平均尺寸是 120~140 mm, 新的容积 CT 在 3~4 步就能够覆盖整个器官。伴随新的数据采集方式, 我们也提出了对应的重建算法, 克服了不完全投影采样的问题, 还进行了广泛的模体和临床实验来阐明所提出方法的有效性。

**关键字:** CT; 心脏成像; 步进-扫描; 锥形束重建